

The impact of Ly α emission line heating and cooling on the cosmic dawn 21-cm signal

Avery Meiksin^{1*}, Piero Madau^{2,3}

¹*SUPA†, Institute for Astronomy, University of Edinburgh, Blackford Hill, Edinburgh EH9 3HJ, UK*

²*Department of Astronomy and Astrophysics, University of California, Santa Cruz, 1156 High Street, Santa Cruz, CA 95064, USA*

³*Institute of Astronomy, University of Cambridge, Madingley Road, Cambridge CB3 0HA, UK*

17 March 2024

ABSTRACT

Allowing for enhanced Ly α photon line emission from Population III dominated stellar systems in the first forming galaxies, we show the 21-cm cosmic dawn signal at $10 < z < 30$ may substantially differ from standard scenarios. Energy transfer by Ly α photons emerging from galaxies may heat intergalactic gas if H II regions within galaxies are recombination bound, or cool the gas faster than by adiabatic expansion if reddened by winds internal to the haloes. In some cases, differential 21-cm antenna temperatures near -500 mK may be achieved at $15 < z < 25$, similar to the signature detected by the EDGES 21-cm cosmic dawn experiment.

Key words: cosmology: theory – dark ages, reionization, first stars – intergalactic medium – radiative transfer – radio lines: general – scattering

1 INTRODUCTION

The first bound stellar systems to form in the Universe have long been believed to be copious emitters of Ly α photons (Partridge & Peebles 1967), possibly in a bright flash brought on by a violent burst of star formation as the first massive stars formed, ionized their surroundings and subsequently exploded as supernovae (Field 1964; Truran & Cameron 1971; Tinsley 1972). The first generation of stars will form through gas processes, and so have very low metallicity. These Population III dominated stellar populations are expected to have an excess of massive stars radiating strongly in the Lyman continuum. Larger Ly α equivalent widths are predicted compared with current galaxies, with values as high as a few thousand Angströms possible (Raiter et al. 2010). While the fraction of star-forming galaxies with strong Ly α emission is observed to decrease at $z > 6$ (eg Stark et al. 2010; Ono et al. 2012; Schenker et al. 2014), this is often interpreted as a consequence of the resonance line scattering of Ly α photons in an increasingly neutral intervening intergalactic medium (IGM) at early epochs (eg Dijkstra et al. 2011).

There is scant direct observational data on star-forming galaxies at $z > 8$. The global rate of Ly α photon production from these systems is consequently unknown, as well as the halo masses in which they may reside. Whilst haloes with masses as low as $\sim 10^6 h^{-1} M_\odot$ may achieve the densities

required to form sufficient molecular hydrogen to cool the halo gas and drive star formation, the UV radiation from the first galaxies at $z > 20$ may dissociate the molecular hydrogen in subsequent generations, suppressing further star formation (Haiman et al. 1997). Star formation would then be restricted to haloes more massive than $\sim 10^7 h^{-1} M_\odot$ that cool through atomic processes. How effective molecular hydrogen dissociation is as a means of suppressing star formation in less massive haloes is currently unknown.

Whilst direct observations of Ly α -emitting galaxies at $z > 20$ are likely somewhat off, such galaxies may have a detectable impact on the 21-cm signature expected from the still neutral IGM (Madau et al. 1997). Under conventional assumptions of star formation in primordial galaxies, with a minimum halo mass of $\sim 10^7 h^{-1} M_\odot$, the metagalactic Ly α photon scattering rate P_α arising from H II regions within the galaxies at $z > 25$ is typically below the thermalization rate P_{th} required to drive the 21-cm spin temperature to the kinetic temperature of the IGM. Strong coupling to the kinetic temperature, with $P_\alpha > 10P_{\text{th}}$, would not be achieved until $z < 20$. As a consequence, only a weak absorption signal against the CMB is expected at $z > 20$, with $|\Delta T_{21\text{-cm}}| < 100$ mK (Barkana & Loeb 2005; Hirata 2006).

In this paper, we show that, allowing for enhanced Ly α photon production in Pop III star H II regions and extending the minimum halo mass for star formation to include molecular hydrogen cooled haloes, the metagalactic Ly α photon background may be boosted at $z > 20$ to a level that substantially alters the predicted strength of the 21-cm signature.

* E-mail: meiksin@ed.ac.uk (AM)

† Scottish Universities Physics Alliance

We also show that for extreme cases of Ly α photon emission, with equivalent widths exceeding 10^5 Å or for haloes emitting to the red of line-centre with moderate equivalent widths but narrow line widths, it may be possible to cool the IGM super-adiabatically, with a 21-cm differential temperature $\Delta T_{21-\text{cm}} < -400$ mK at $15 < z < 26$, similar to the recent signal reported for the EDGES global 21-cm signature experiment (Bowman et al. 2018). Whether such extreme conditions may be realized in astrophysical sources, however, is unknown.

This paper is organized as follows. In the next section, the possible level of Ly α emission from primordial galaxies is assessed. In Sec. III, we describe the method for solving for the metagalactic Ly α radiation field from the sources. Solutions for the resulting evolution of the IGM kinetic temperature are presented in Sec. IV, allowing for Ly α photon recoil heating and cooling of the IGM. The results are discussed in Sec. V, and we summarize our conclusions in Sec. VI. We adopt a flat Λ CDM cosmological model with $\Omega_m = 0.3111$, $\Omega_b h^2 = 0.02242$, $h = 0.6766$, $\sigma_8 = 0.8102$ and spectral index $n = 0.9665$ (Planck Collaboration 2018). A comoving kiloparsec is designated ‘ckpc.’

2 Ly α PHOTON SOURCES

2.1 Emergent Ly α emission from primordial star-forming galaxies

We consider three varieties of Ly α photons produced by star-forming galaxies: (a) directly produced Ly α photons from H II regions within the galaxies, (b) continuum photons which redshift to the local Ly α resonance frequency as a result of cosmological expansion, and (c) continuum photons which redshift to higher order Lyman transitions that produce Ly α photons through radiative cascades. Averaged over cosmological scales, the first type dominates, as we shall discuss in this section. We begin by characterising the emission line profiles emergent from the galaxies.

In a metal-free environment, a minimum halo mass between $10^5 - 10^7 M_\odot$ is required to form stars at $z > 15$ in a Cold Dark Matter dominated cosmology following molecular hydrogen production through gaseous processes and cooling (Bond & Szalay 1983; Blumenthal et al. 1984; Couchman & Rees 1986; Yoshida et al. 2003). Because of the relative streaming velocity between baryons and dark matter at the recombination era, however, the gas content of lower mass haloes is suppressed (Tseliaxhovich & Hirata 2010). Although estimates vary, the lowest mass haloes allowing substantial star formation likely exceeds $\sim 10^6 h^{-1} M_\odot$ (eg Visbal et al. 2012; Schauer et al. 2019).

The typical central hydrogen density and temperature of a $10^6 M_\odot$ halo collapsing at $z = 20$ are $n_H \simeq 10 \text{ cm}^{-3}$ and $T \simeq 10^3$ K, respectively, within a core comoving radius $r_c \simeq 3 \text{ ckpc}$ (eg Meiksin 2011). The formation of H II regions around the more massive stars will produce Ly α photons. If dust absorption is low, the Ly α photons will scatter until they escape the galaxy. Because the interstellar medium (ISM) of the galaxies will typically be highly optically thick to Ly α photons, the emitted profile will be double-peaked about the line centre, as the Ly α photons scatter in frequency until they are sufficiently removed from line centre to escape (Zanstra 1949; Harrington 1973).

An exception to the double-peaked profile may arise if the ISM is expanding, as in a wind powered by hot stars or supernovae. In this case the profile may be highly reddened. Such reddened Ly α profiles are common in star-forming galaxies (eg Steidel et al. 2010; Heckman et al. 2011). Numerical simulations suggest the halo gas may become highly rarefied following expulsion of most of the gas by supernovae, and cooling may lower the gas temperature to below 1000 K (Whalen et al. 2008, 2013; Smith et al. 2015). In such circumstances, the reddened profile may peak only several Doppler widths to the red of line centre. We shall see below such sources can cool the IGM if their combined intensity is sufficiently strong. Both double-peaked and reddened emergent Ly α profiles are considered.

2.2 Metagalactic Ly α photon scattering rate

We quantify the Ly α emission intensity from the galaxies in terms of the metagalactic Ly α scattering rate per hydrogen atom they produce. For a specific number density n_ν of Ly α photons, the Ly α photon scattering rate per atom in the lower state is

$$P_\alpha = \sigma_\alpha c \int_0^\infty d\nu \varphi_V(\nu) n_\nu, \quad (1)$$

where the total scattering cross section is $\sigma_\alpha = (\pi e^2 / m_e c) f_\alpha$ with upper oscillator strength f_α and $\varphi(\nu)$ is the Voigt scattering profile. The characteristic scattering rate for which Ly α photons couple the spin temperature of the 21-cm hyperfine transition to the light temperature instead of to the CMB temperature through the Wouthuysen-Field mechanism (Wouthuysen 1952; Field 1958) is given by the thermalization scattering rate

$$P_{\text{th}} = \frac{27 A_{10} T_{\text{CMB}}(z)}{4 T_*} \simeq (1.6 \times 10^{-11} \text{ s}^{-1}) \left(\frac{1+z}{21} \right), \quad (2)$$

(Madau et al. 1997). Here, A_{10} is the spontaneous decay rate of the 21-cm transition and $T_* = h\nu_{10}/k$ is the temperature corresponding to the 21-cm transition of frequency ν_{10} . For $P_\alpha \gg P_{\text{th}}$, the spin temperature will track the light temperature, which will be close to the kinetic temperature of the IGM (Field 1959; Meiksin 2006).

To maintain a scattering rate P_α in an IGM with a Sobolev parameter $\gamma_S = H(z)\nu_0/(\bar{n}_H \sigma_\alpha c)$, where ν_0 is the Ly α photon resonance frequency, $H(z)$ is the Hubble parameter and \bar{n}_H the average intergalactic hydrogen density, Ly α photons must be generated at the rate

$$\dot{n}_\alpha = \gamma_S \bar{n}_H P_\alpha \quad (3)$$

(Field 1959; Meiksin 2010). For a net efficiency ϵ_{SF} for converting gaseous baryons in haloes into nuclear fuel within stars, allowing $L_{\text{Ly}\alpha} = f_{\text{Ly}\alpha} L_{\text{bol}}$ where L_{bol} is the stellar bolometric luminosity, with $f_{\text{Ly}\alpha} \simeq 0.2 - 0.4$ for low metallicity (Pop III) stars with a Salpeter stellar initial mass function (Raiter et al. 2010), and an energy generation rate per unit mass $0.007 c^2$ for nuclear burning, the total generation rate of Ly α photons integrated over halo masses is:

$$\dot{n}_\alpha = (0.001 - 0.003) \frac{\epsilon_{\text{SF}}}{e_\alpha} \frac{\Omega_b}{\Omega_m} \frac{d}{dt} \int_{M_{\text{min}}} dM_h \frac{dn_h(M_h)}{dM_h} M_h c^2, \quad (4)$$

for a differential number density of halos $dn_h(M_h)/dM_h$,

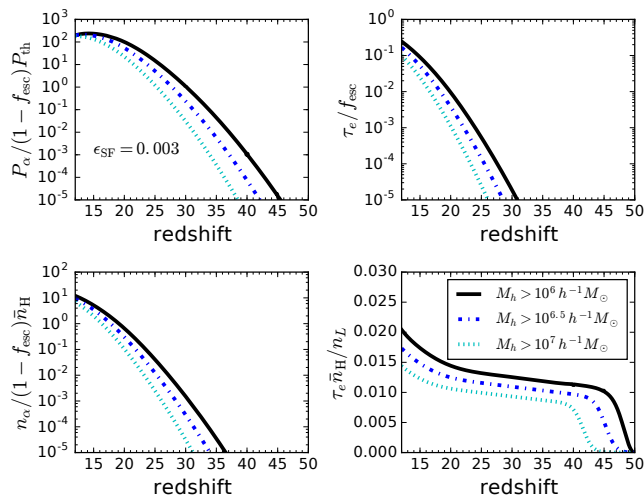


Figure 1. Evolution of the Ly α scattering rate P_α , normalized by the thermalization rate P_{th} (top left panel), integrated number density n_α of Ly α photons produced, normalized by the mean IGM hydrogen density \bar{n}_H (bottom left panel), evolution of the Thomson optical depth (top right panel), and of the Thomson optical depth scaled to n_L/\bar{n}_H , where n_L is the number of Lyman continuum photons produced in the IGM for $f_{\text{esc}} > 0$ (bottom right panel). A fiducial baryon conversion efficiency of $\epsilon_{\text{SF}} = 0.003$ is assumed. The curves correspond to the indicated minimum halo mass cut-off values for star formation.

minimum halo mass M_{min} for forming stars, and Ly α photon energy e_α . Typically, $\epsilon_{\text{SF}} \simeq 0.001 - 0.01$.¹ The corresponding Ly α equivalent widths range over 400 – 2000 Å for continuous star formation and 2000 – 4000 Å for a young burst population (Raiter et al. 2010), with the higher values corresponding to an extended upper stellar mass of $500 M_\odot$, and truncating the lower end at $50 M_\odot$ for the highest values.

The Ly α scattering rate evolves rapidly, as shown in Fig. 1. Depending on the minimum halo mass for producing stars, by $z \approx 25 - 35$, the scattering rate exceeds the thermalization rate and the Ly α photons are able to couple the spin temperature to the gas temperature. The cumulative number density of Ly α photons produced rises rapidly as well, because of the rapid evolution in the number of haloes above the threshold mass, potentially exceeding the mean number of intergalactic hydrogen atoms by $z \approx 20$. Such a high number is problematic in terms of reionization of the IGM, because the production rate of Lyman continuum photons from the stars is comparable to the production rate of Ly α photons in H II regions. A Ly α photon flux sufficient to provide moderate coupling of the IGM spin temperature to the kinetic temperature requires an escape fraction $f_{\text{esc}} \lesssim 0.2$ of ionizing radiation from the galaxies (Madau 2018).

Details of the relation between the Ly α scattering rate and reionization limits are discussed in the Appendix. There it is shown that, for an escape fraction $f_{\text{esc}} < 0.2$, requir-

ing $n_L/\bar{n}_H < 0.5$ imposes the restriction $P_\alpha/P_{\text{th}} \lesssim 200$ for $\epsilon_{\text{SF}} = 0.003$. Even for the extreme efficiency $\epsilon_{\text{SF}} = 0.1$, $P_\alpha/P_{\text{th}} < 3000$ is required, while for $\epsilon_{\text{SF}} = 10^{-4}$, $P_\alpha/P_{\text{th}} < 20$ is required. The limits become even more severe for higher escape fractions.

2.3 Ly α photon heating of the IGM

The required metagalactic Ly α photon scattering rate to alter the thermal evolution of the IGM may be quantified as follows. For a Ly α photon number density n_ν , the volumetric heating rate of the IGM resulting from atomic recoils is

$$G_H = P_\alpha n_H \frac{h\nu_0}{m_H c^2} h\nu_0 \left(1 - \frac{T_K}{T_L}\right), \quad (5)$$

(Meiksin 2006), where m_H is the mass of a hydrogen atom, T_K is the IGM kinetic temperature and T_L is the light temperature of the Ly α radiation field (see below). The limit $T_K \ll T_L$ of Eq. (5) recovers the heating rate given by Madau et al. (1997). At lower light temperatures, the heating rate is modified by the factor $1 - T_K/T_L$, which could result either in net heating or cooling (cf Chen & Miralda-Escudé 2004; Chuzhoy & Shapiro 2006).

To change the gas temperature within a Hubble time requires a heating rate $G_H(2/3H) > (3/2)n_H k_B T_K$, or a scattering rate

$$P_\alpha > \frac{9}{8} H(z) \epsilon^{-2} \left(1 - \frac{T_K}{T_L}\right)^{-1}, \quad (6)$$

where $\epsilon = h\nu_0/(2kT_K m_H c^2)^{1/2} \simeq 0.025 T_K^{-1/2}$ is the recoil parameter. In a standard cosmological expansion scenario, the diffuse IGM temperature at $z = 20$ is $T_K \simeq 10$ K (Seager et al. 2000). We shall show that typically $|1 - T_K/T_L| \sim 10^{-4} - 10^{-3}$. Then the required Ly α scattering rate is

$$\begin{aligned} P_\alpha &> (2.2 \times 10^{-9} \text{ s}^{-1}) \frac{T_K}{10 \text{ K}} \left(10^3\right) \left(1 - \frac{T_K}{T_L}\right)^{-1} \\ &= (10^2 - 10^3) P_{\text{th}}. \end{aligned} \quad (7)$$

Additional Ly α photons are provided by cascades from higher order Lyman photon scattering produced by continuum source photons redshifting into higher order Lyman resonances (Barkana & Loeb 2005). Higher order Lyman photons scattering within the Doppler core will also heat the gas near the sources. The cascade-produced Ly α photons and higher order Lyman photon heating are accounted for following Meiksin (2010). Details are provided in an Appendix.

3 THE METAGALACTIC Ly α RADIATION BACKGROUND

The heating rate by Ly α photons is sensitive to the shape of the metagalactic Ly α radiation background. We solve for the frequency dependence of the radiation field in the diffusion approximation. We shall consider both directly emitted Ly α photons from galaxies and continuum photons that redshift to the local Ly α frequency. At $z = 20$, the comoving density of haloes more massive than $10^6 h^{-1} M_\odot$ is $\sim 140 \text{ cMpc}^{-3}$ (Reed et al. 2007), corresponding to a mean comoving separation of $\lesssim 200 \text{ ckpc}$. For comparison, the mean-free-path

¹ Setting $\epsilon_{\text{SF}} = f_*/3$, where f_* is the conversion efficiency of gas mass in haloes to stellar mass, and adopting a Pop II value of $f_{\text{Ly}\alpha} = 0.03$ and nebular Ly α equivalent width of 200 Å (Raiter et al. 2010), matches the number of photons produced per stellar baryon by the stellar continuum between Ly α and Ly β of ~ 6500 given by Barkana & Loeb (2005).

of Ly α photons in the IGM even up to 100 Doppler widths from line centre is much smaller, ~ 15 ckpc, so that the Ly α radiation field surrounding the galaxies may be treated in the diffusion approximation for both directly emitted Ly α photons and those arising from the redshifted galaxy continua. The photons diffuse through the IGM on scales up to ~ 1 Mpc (proper, independent of redshift) before free-streaming becomes important (Loeb & Rybicki 1999; Higgins & Meiksin 2012). This corresponds to a region containing $10^6 - 10^7$ haloes more massive than $10^6 M_\odot$. The large number of galaxies within the diffusive region of the Ly α photons ensures a smoothly varying radiation field throughout the IGM. Accordingly, the galactic sources of Ly α photons will be treated as isotropic and homogeneously spatially distributed.

In a homogeneous and isotropic expanding medium, the radiative transfer equation for the specific comoving number density $n(\nu, t)$ of Ly α photons of frequency ν at time t produced by a comoving source density $S(\nu, t)$ is solved in the diffusion approximation for a homogeneous and isotropic radiation field. Defining the dimensionless frequency shift $x = (\nu - \nu_0)/\Delta\nu_D$, where ν_0 is the Ly α resonance transition frequency, $\Delta\nu_D = \nu_0(2kT/m_H)^{1/2}/c$ is the Doppler width, a conformal time $\tau = \int_0^t dt n_H(t) \sigma_\alpha c / \Delta\nu_D$ for neutral hydrogen density n_H , and the dimensionless Voigt profile $\phi_V(x) = \varphi_V(\nu) \Delta\nu_D$, the diffusion equation takes the dimensionless form

$$\begin{aligned} \frac{\partial n_x(\tau)}{\partial \tau} &= \frac{\partial \log \Delta\nu_D}{\partial \tau} n_x(\tau) \\ &= \frac{1}{2} \frac{\partial}{\partial x} \left\{ 2[\epsilon \phi_V(x) + \gamma_S] n_x(\tau) + \phi_V(x) \frac{\partial}{\partial x} n_x(\tau) \right\} \\ &+ \tilde{S}(x, \tau), \end{aligned} \quad (8)$$

(Rybicki & dell’Antonio 1994; Chen & Miralda-Escudé 2004; Meiksin 2006), where $n_x(\tau) = n_\nu(t) \Delta\nu_D$ and $\tilde{S}(x, \tau) = S(\nu) (\Delta\nu_D)^2 / (n_H \sigma_\alpha c)$ have been defined, a possible time-evolution of $\Delta\nu_D$ has been allowed for and terms of order xb/c have been neglected. The recoil parameter ϵ accounts for atomic recoil after collision with a Ly α photon. The valid recovery of the effects of atomic recoil at this level of approximation requires $b/c \ll 2\epsilon$, or $T \ll h\nu_0/k \approx 10^5$ K for hydrogen Ly α photons.

At low temperatures ($T < 4$ K), corrections to the radiative transfer equation arising from the fine structure of the Ly α resonance and spin-flip scatterings start to become relevant (Hirata 2006). These lead to corrections to the recoil parameter and effective Ly α scattering rate. The correction factor for the recoil parameter depends on the spin temperature, given by

$$T_S = \frac{T_{\text{CMB}} + y_\alpha T_L + y_c T_K}{1 + y_\alpha + y_c}, \quad (9)$$

where y_α and y_c are weight factors depending on the Ly α and collisional de-excitation rates (Field 1959; Madau et al. 1997; Meiksin 2006). Since we shall investigate the case of strong Ly α scattering, Eq. (9) shows the spin temperature goes over to the IGM kinetic temperature, since the light temperature quickly converges to the kinetic temperature (Meiksin 2006), resulting in a negligible change to the recoil parameter. In this limit, the Ly α scattering rate may be adjusted by reducing the Sobolev parameter by the factor $1 + 0.4/T_K$ (Chuzhoy & Shapiro 2006). The effect on the

21-cm differential temperatures in the contexts we examine is very small.

The left hand side of Eq. (8) is of order $(H\lambda_{\text{mfp}}/c)n_x$, much smaller than the right hand side, except possibly far in the wings. Accordingly, the number density of photons may be taken as time-steady in the comoving frame. The diffusion approximation then becomes

$$\begin{aligned} \phi_V(x) \frac{\partial}{\partial x} n_x(\tau) &+ 2\epsilon \phi_V(x) n_x(\tau) + 2\gamma_S n_x(\tau) \\ &= -2 \int_{-\infty}^x dx' \tilde{S}(x', \tau) + 2\gamma_S n_{-\infty}(\tau) \end{aligned} \quad (10)$$

where $2\gamma_S n_{-\infty}(\tau)$ is an integration constant. The source function and boundary conditions on $n_x(\tau)$ satisfy the integral constraint

$$\int_{-\infty}^{\infty} dx \tilde{S}(x, \tau) = \gamma_S [n_{-\infty}(\tau) - n_\infty(\tau)] \quad (11)$$

given by the asymptotic values of the radiation field. In the absence of a source, the asymptotic values correspond to a flat background continuum, with $n_\infty = n_{-\infty}$.

Allowing for both a source and a background continuum is readily accommodated by fixing n_∞ to the continuum value, arising from the continuum emission from galaxies. Because continuum photons emitted between Ly α and Ly β redshift to local Ly α photons, a source that injects the same number of Ly α photons directly will have an equivalent width of $\lambda_\alpha - \lambda_\beta \simeq 190$ Å. Sources with Ly α equivalent widths of 1000 – 3000 Å will then produce 5–15 times as many Ly α photons directly as produced by the continuum. Additional Ly α photons may also be produced from higher energy continuum photons that redshift to higher order Lyman resonances where they are scattered and subsequently cascade to Ly α photons (Chen & Miralda-Escudé 2004).

The light temperature in Eq. (5) is given by

$$T_L = \int_0^\infty dx n_x \phi_V(x) / \int_0^\infty dx n_x \phi_V(x) \frac{1}{T_n(x)}, \quad (12)$$

(Meiksin 2006), where

$$T_n(x) = -\frac{h\Delta\nu_D}{k} \left(\frac{d \log n_x}{dx} \right)^{-1} \quad (13)$$

(cf Rybicki 2006). Using Eq. (10), the light temperature may be expressed in the often numerically more practical alternative form

$$\begin{aligned} T_L &= -\frac{h\Delta\nu_D}{k} \int_{-\infty}^{\infty} dx \phi_V(x) n_x \\ &\times \left\{ \int_{-\infty}^{\infty} dx \left[2\gamma_S (n_{-\infty} - n_x) - 2 \int_{-\infty}^x dx' \tilde{S}(x') \right] \right. \\ &\left. - 2\epsilon \int_{-\infty}^{\infty} dx \phi_V(x) n_x \right\}^{-1} \end{aligned} \quad (14)$$

(cf Chen & Miralda-Escudé 2004). In a static medium, T_L rapidly converges to T_K , resulting in no net heating or cooling (Meiksin 2006). By contrast, in a dynamical medium the light temperature may never reach the kinetic temperature, resulting in a non-vanishing heating or cooling rate (Chen & Miralda-Escudé 2004).

The kinetic temperature T_K of the IGM evolves according to

$$\frac{dT_K}{dz} = -\frac{2}{1+z}T_K - \frac{2}{3} \frac{1}{(1+z)H(z)} \frac{G_H}{nk}, \quad (15)$$

for particle density $n \simeq 1.1n_H$, allowing for helium and taking the IGM to be almost entirely neutral.

The measured differential 21-cm antenna temperature between the IGM spin temperature at the mean IGM density and the CMB is

$$\delta T_{21-\text{cm}} = (1+z)^{-1} [T_S(z) - T_{\text{CMB}}(z)] [1 - e^{-\tau_{21}(z)}], \quad (16)$$

where the intergalactic 21-cm optical depth is

$$\tau_{21}(z) \simeq 0.402 \frac{x_{\text{HI}}(z)}{T_S(z)} \left(\frac{1+z}{13} \right)^{1.5}, \quad (17)$$

(Madau et al. 1997), and $x_{\text{HI}}(z)$ is the neutral fraction at redshift z .

4 EVOLUTION OF DIFFERENTIAL 21-CM ANTENNA TEMPERATURE

4.1 Static ISM models

The impact of the emergent Ly α radiation from galaxies on the differential 21-cm antenna temperature depends both on the intensity of the radiation and its thermal influence on the IGM through atomic recoils. The scattering of Ly α photons through a static ISM splits the Ly α line into a characteristic double-lobed profile, with horns symmetrically placed to the red and blue of line centre. To estimate the amount of heating by these Ly α photons, the Ly α emission line is approximated using the emergent flux from a static slab,

$$\tilde{S}(x_s) = \frac{1}{6^{1/2}} \pi \gamma_S n_{-\infty} \frac{x_s^2}{a\tau_0} \frac{1}{\cosh[\exp((\pi^2/6)(2/3)^{1/2} x_s^3/(a\tau_0))]}, \quad (18)$$

(Harrington 1973), where $x_s = (\nu - \nu_\alpha)/\Delta\nu_D(T_s)$ for a slab of temperature T_s , as shown in Fig. 2 (top left panel). The source function has been normalized according to

$$\int_{-\infty}^{x_s} dx'_s \tilde{S}(x'_s) = \frac{2}{\pi} \gamma_S n_{-\infty} \text{atan} \left[\exp \left(\frac{\pi^2}{6} \left(\frac{2}{3} \right)^{1/2} \frac{x_s^3}{a\tau_0} \right) \right], \quad (19)$$

which satisfies the integral constraint Eq (11) in the absence of a background continuum ($n_\infty = 0$). (When required, the source is appropriately renormalized in the presence of continuum produced Ly α photons to satisfy the integral constraint.)

On solving for the radiative transfer of the source photons using Eq. (10), the blue horn is found to produce a (nearly) flat Ly α continuum across line centre (cf Higgins & Meiksin 2009), which heats the IGM through Ly α recoils. The evolution of the IGM temperature and differential 21-cm antenna temperature for haloes with total masses $M_h > 10^6 h^{-1} M_\odot$ is shown in Fig. 2. Emission through a neutral hydrogen column density of 10^{18} cm^{-2} with temperature $T_{\text{ISM}} = 10^4 \text{ K}$ is assumed, characteristic values for a Strömgren region (see the Appendix). The heating by Ly α photon recoils increases the IGM temperature T_K by $z < 21$ (top right panel). For comparison, the IGM temperature with no heating is shown as the black dotted line, which decreases monotonically with decreasing redshift, in contrast

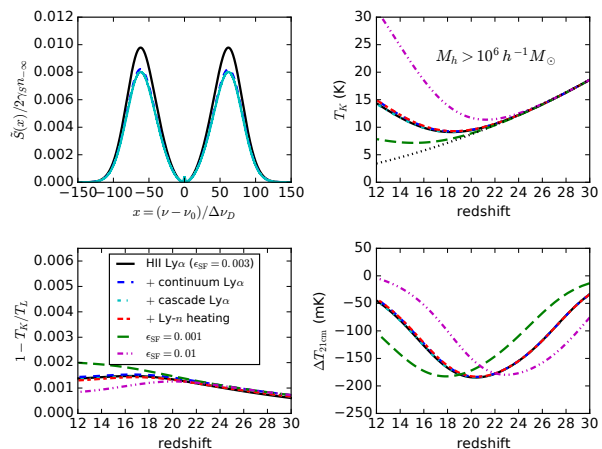


Figure 2. Slab source function at $z = 30$ (top left) and evolution of the IGM temperature T_K (top right), heating efficiency factor $1 - T_K/T_L$, where T_L is the light temperature (lower left), and the differential 21-cm antenna temperature $\Delta T_{21\text{cm}}$ (lower right) for emission from haloes with total masses $M_h > 10^6 h^{-1} M_\odot$. Internal scattering in the sources through a neutral hydrogen column density of 10^{18} cm^{-2} with temperature $T_{\text{ISM}} = 10^4 \text{ K}$ is assumed.

to the upturn in the models with heating. Results are shown for Ly α emission line photons produced in the H II regions of stars forming within the haloes with an equivalent width of 1000 \AA for a star formation efficiency $\epsilon_{\text{SF}} = 0.003$ (black solid lines).

An allowance for additional Ly α photons from redshifted continuum radiation, normalized to an H II region produced Ly α equivalent width of 1000 \AA , slightly enhances the heating (blue dashed lines). The volume-averaged enhancement in the number of Ly α photons produced through radiative cascades in the IGM is found to be only 14 percent, and results in a slight reduction in the heating rate, approximately cancelling the heating produced by redshifted continuum Ly α photons (cyan dot-dot-dashed lines). Continuum photons redshifted into higher order Lyman resonances are found to increase the heating rate over the H II region produced Ly α photons by 8 – 10 percent, approximately cancelling the cooling by the cascade-produced Ly α photons and nearly restoring the continuum Ly α photon heating rate (red short-dashed-long-dashed lines). In the remainder of this paper, the effects of higher order Lyman photons is neglected.

Results for models with $\epsilon_{\text{SF}} = 0.001$ (green long dashed lines) and 0.01 (magenta dot-dot-dashed lines) are also shown. All the models produce a distinctive dip in the 21-cm brightness temperature as a function of redshift (bottom right panel). The Ly α recoil heating efficiency factor $1 - T_K/T_L$ is only weakly sensitive to ϵ_{SF} (lower left panel).

Allowing for minimal halo masses for star formation between $10^6 - 10^7 h^{-1} M_\odot$ shifts the onset of heating, as shown in Fig. 3. A star formation efficiency of $\epsilon_{\text{SF}} = 0.003$ is assumed, and the Ly α photons scatter through a column density $N_{\text{HI}} = 10^{18} \text{ cm}^{-2}$ at $T_{\text{ISM}} = 10^4 \text{ K}$. The differential 21-cm antenna temperature reaches a minimum of $\Delta T_{21-\text{cm}} \simeq -200 \text{ mK}$, shifting gradually from $z \lesssim 24$ to 17 as the minimum halo mass increases.

For non-zero escape fractions of ionizing radiation, a

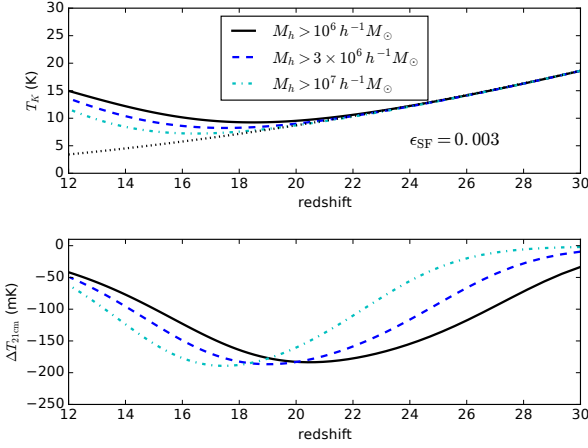


Figure 3. Evolution of the IGM temperature T_K (top panel) and the differential 21-cm antenna temperature $\Delta T_{21\text{cm}}$ (lower panel) for minimal halo masses between $M_h = 10^6 h^{-1} M_\odot$ and $10^7 h^{-1} M_\odot$. The star formation efficiency is $\epsilon_{\text{SF}} = 0.003$. Internal scattering in the sources through a neutral hydrogen column density of 10^{18} cm^{-2} with temperature $T_{\text{ISM}} = 10^4 \text{ K}$ is assumed.

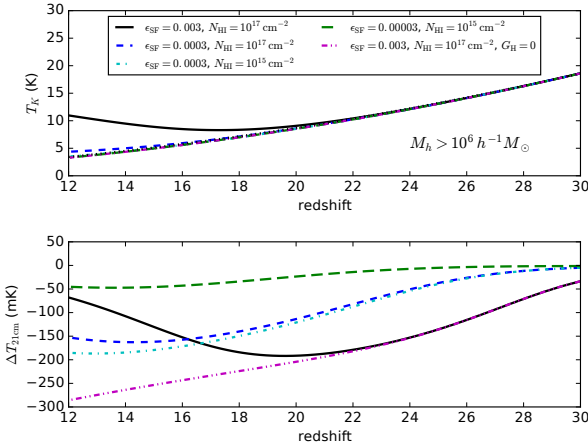


Figure 4. Evolution of the IGM temperature T_K (top panel) and the differential 21-cm antenna temperature $\Delta T_{21\text{cm}}$ (lower panel) for a minimal halo mass $M_h > 10^6 h^{-1} M_\odot$, star formation efficiency $\epsilon_{\text{SF}} = 0.00003$ to 0.003 , and internal scattering in the sources through a neutral hydrogen column density of $10^{15} - 10^{17} \text{ cm}^{-2}$. A slab temperature $T_{\text{ISM}} = 10^4 \text{ K}$ is assumed.

Strömgren sphere may not form around the star-forming regions within the galaxies. In this case, the H I column density through which the Ly α photons scatter need not be as high as 10^{18} cm^{-2} . Decreasing the column density to 10^{17} cm^{-2} slightly lowers the differential antenna temperature, as shown in Fig. 4 (black solid lines). Since the Ly α production rate was not altered, a lower H I column density has the equivalent effect of an enhanced level of Ly α production compared with the case of a vanishing escape fraction of ionizing radiation. This is because the blue lobe of the emergent Ly α spectrum moves closer to line centre and the photons no longer heat the gas through recoils as efficiently.

By contrast, lowering the star formation rate, and so the Ly α production rate, by an order of magnitude reduces the amount of heating by Ly α photon recoils as well as the

degree of coupling to the IGM temperature, resulting in a shallower trough in $\Delta T_{21-\text{cm}}$ (short-dashed blue lines).

Decreasing the H I column density to 10^{15} cm^{-2} has little additional effect (cyan dot-dashed lines). It does, however, introduce net cooling at $z > 18.5$, as the redward peak in the Ly α emission profile through the slab now moves closer to line centre. Cooling by recombinant Ly α emission line photons produced within the H II regions now exceeds the heating by continuum-produced Ly α photons. The amount of cooling is slight, lowering the IGM temperature to $T_K = 7.4 \text{ K}$, compared with the adiabatic cooling value of 7.6 K . Decreasing the star formation efficiency by another order of magnitude produces a very shallow dip in the 21-cm differential antenna temperatures (green long-dashed lines). For all the models, by $z < 18$, the differential antenna temperature lies well above the minimum level allowing only for adiabatic expansion and complete coupling of the spin temperature to the IGM temperature, which approaches $\Delta T_{21-\text{cm}} \gtrsim -300 \text{ mK}$ by $z = 12$ (magenta dot-dot-dashed lines).

4.2 Expanding ISM models

Observed spectra of Ly α -emitting star-forming galaxies often exhibit distorted Ly α profiles with a dominant redward peak (eg Steidel et al. 2010; Heckman et al. 2011), consistent with an outflow interpretation (Verhamme et al. 2012; Smith et al. 2015). The outflow velocities are typically in excess of 100 km s^{-1} . The velocity offset decreases with inferred halo mass; extrapolating the trend to low mass haloes corresponds to $4 - 7 \text{ km s}^{-1}$ for halo masses $10^6 - 10^7 h^{-1} M_\odot$ (Mason et al. 2018).

Such low values, however, may not be realizable for Ly α photons originating in H II regions. The Doppler broadening alone is 13 km s^{-1} for gas at 10^4 K . The flux of Ly α photons scattering through a typical Strömgren sphere H I column density of 10^{18} cm^{-2} peaks at $\sim 35 \text{ km s}^{-1}$ on the blue and red sides of line centre (Harrington 1973). An outflow velocity comparable to the halo escape velocities would little shift the peaks redward, so that the 21-cm signature would be similar to the static slab model considered above.

If, however, a residual strong wind subsided to an outflow velocity of $\sim 50 \text{ km s}^{-1}$, then the blue-most peak would be shifted to $\sim 15 \text{ km s}^{-1}$ to the red of line centre. We approximate the resulting Ly α photon emission profile using the homogeneous outflow solution in the diffusion approximation of Loeb & Rybicki (1999). This model assumes a point source with a δ -function frequency profile centred in the red Lorentz wing of Ly α . The Ly α photons scatter in an infinite homogeneous ISM expanding isotropically about the source. We approximate the emergent Ly α emission from a halo using the flux at a given radius R_w representing the edge of the halo, with a linear velocity profile out to the edge $v = v_w(r/R_w)$. The source function for a source number density n_s is then

$$S_\nu = n_s (4\pi R_w)^2 H_\nu \quad (20)$$

where the specific flux H_ν is related to the angle-averaged intensity J_ν and ISM inverse attenuation length χ_ν by $H_\nu = -(\partial J_\nu / \partial r) / (3\chi_\nu)$. It is convenient to express the solution using the dimensionless frequency and distance variables $\tilde{\nu} = (\nu_\alpha - \nu) / \nu_*$ and $\tilde{r} = r / r_*$, respectively, where

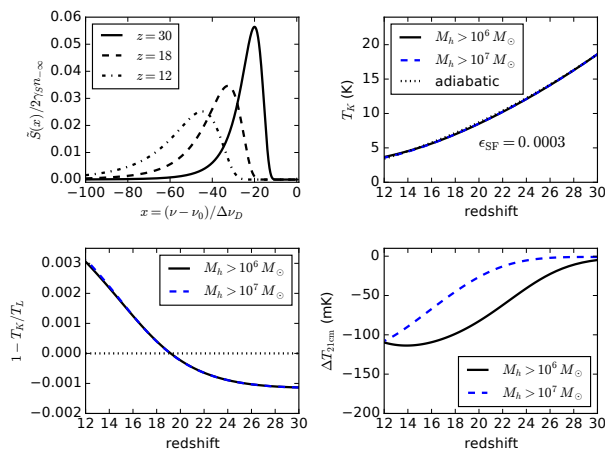


Figure 5. Outflow source function (top left) and resulting evolution of the IGM temperature T_K (top right), heating efficiency factor $1 - T_K/T_L$, where T_L is the light temperature (lower left), and the differential 21-cm antenna temperature $\Delta T_{21-\text{cm}}$ (lower right) for emission from haloes with total masses $M_h > 10^6$ and $10^7 h^{-1} M_\odot$. Internal scattering in the sources through a neutral hydrogen density of 10^{-4} cm^{-3} with temperature $T_{\text{ISM}} = 110 \text{ K}$, an outflow region extending to $R_w = 200 \text{ pc}$ and maximum outflow velocity $v_w = 7 \text{ km s}^{-1}$ are assumed.

$\nu_* = \sigma_\alpha A_\alpha \lambda_\alpha n_{\text{HI}} / (4\pi^2 dv/dr)$ and $r_* = \lambda_\alpha \nu_* / (dv/dr)$. At $r > r_*$, the diffusion approximation begins to break down and the Ly α photons start to free stream (Loeb & Rybicki 1999; Higgins & Meiksin 2012). The dimensionless flux is then

$$\tilde{H}_\nu = \frac{3\tilde{r}}{8\pi\tilde{\nu}} \left(\frac{9}{4\pi\tilde{\nu}^3} \right)^{3/2} e^{-9\tilde{r}^2/4\tilde{\nu}^3}. \quad (21)$$

We normalize the comoving source by

$$\int_{-\infty}^{x_w} dx'_w \tilde{S}(x'_w) = \frac{2}{\pi^{1/2}} \gamma_S n_{-\infty} \gamma\left(\frac{3}{2}, t\right), \quad (22)$$

where $x_w = (\nu - \nu_\alpha) / \Delta\nu_D (T_w)$ for an ISM temperature T_w in the expanding wind, $t = -(\nu_* / \Delta\nu_D)^3 9\tilde{R}_w^2 / 4x^3$, $\gamma(a, t)$ is an incomplete gamma function and $x < 0$. The peak of the emergent flux is at

$$-x_{\text{peak}} = \frac{3}{22^{1/3}} \left(\frac{R_w}{r_*} \right)^{2/3} \frac{\nu_*}{\Delta\nu_D}. \quad (23)$$

Several criteria must be satisfied for the validity of the expanding wind solution: (1) the emission peak must lie in the Lorentz wing, (2) the mean free path at the emission peak must be smaller than R_w , and (3) the wind region must satisfy $R_w < r_*$.

Results from numerical simulations show the gaseous contents of the haloes of primordial galaxies to be highly dynamic. The first supernovae in a halo will expel the halo gas in a wind. The hydrogen density may be lowered to values below 10^{-4} cm^{-3} with temperatures cooling to $100 - 1000 \text{ K}$ (Whalen et al. 2008, 2013; Smith et al. 2015). Subsequently, gas that has not escaped may refill the haloes, resulting in a back flow and re-establishing hydrogen densities of $\sim 1 \text{ cm}^{-3}$. Inflow from mergers will also contribute to the restoration of the gaseous contents. These effects are still poorly understood, with no direct observations.

For a neutral hydrogen density 1 cm^{-3} and temperature

10^4 K in a halo with a linear outflow velocity profile reaching 50 km s^{-1} at $R_w = 100 \text{ pc}$, $x_{\text{peak}} \simeq -670$ for an IGM temperature of 18 K . Such a redward peak will have little effect on the IGM; the interaction between the sources and the IGM will be dominated by the source continua. Lowering the H I density to as low as 0.004 cm^{-3} (holding the halo gas temperature and flow parameters fixed), still results in a peak at $x_{\text{peak}} \simeq -110$. Lower densities violate the conditions required for the diffusion approximation.

In the absence of a high H I column density, a large outflow velocity is no longer required for validity of the expansion solution. For a 200 pc radius with an expansion velocity of 7 km s^{-1} , on the order of a halo escape velocity, a hydrogen density of 10^{-4} cm^{-3} and ISM temperature of 110 K results in $x_{\text{peak}} \simeq 16 - 40$ over $z = 30$ to 12 . (Too high an ISM temperature, exceeding 600 K , results in a peak within the Doppler core.) The absence of a high H I column density, however, requires a low Ly α photon production rate to ensure the escaping Lyman continuum (LyC) radiation does not overly ionize the IGM (see Fig. 1).

Results are shown in Fig. 5 for $\epsilon_{\text{SF}} = 0.0003$ and a Ly α equivalent width of $W = 1000 \text{ \AA}$ relative to the continuum. The strong red peak in the source function initiates cooling of the IGM by Ly α scattering (lower left panel), with the IGM temperature decreasing slightly faster than given by adiabatic expansion alone, but at most by about 5 percent (top right panel). Because the IGM temperature decreases with time (from cooling both by Ly α recoils and adiabatic expansion), the peak in the source function shifts increasingly towards the red, reducing the strength of the cooling. By $z \simeq 19$, recoil heating by the Ly α continuum dominates. Despite the lower IGM temperatures, the differential 21-cm absorption signature (lower right) is weaker than for the static slab models considered above because the Ly α scattering rate is smaller.

4.3 Super-adiabatic cooling models

The Ly α scattering induced cooling in Fig. 5 illustrates that the reddened Ly α radiation spectrum in an expanding ISM is able to cool the IGM faster than adiabatic expansion alone. The cooling rate is limited by the requirement that the escaping LyC radiation from the source population does not overly photoionize the IGM; it is not limited by the Ly α photon flux. Motivated by the low differential 21-cm antenna temperatures reported from the EDGES experiment (Bowman et al. 2018), we explore how large a cooling rate by Ly α photon recoil scattering may be achieved, presuming a low intrinsic level of LyC ionizing radiation.

In Fig. 6, the IGM temperature and differential 21-cm antenna temperature evolution are shown for a star formation efficiency $\epsilon_{\text{SF}} = 0.0003$, for which the LyC radiation from haloes with masses exceeding $10^6 h^{-1} M_\odot$ would not be sufficient to photoionize the IGM at a level in conflict with CMB limits on the intergalactic Thomson optical depth. The same cool, low density slowly expanding internal environment is assumed for the haloes as in Sec. 4.2.

Results are shown for a central source producing Ly α emission line photons with equivalent width values in the range $W = 10^3 - 10^6 \text{ \AA}$. A value of 4000 \AA is at the upper end of plausible Ly α equivalent widths produced by H II regions ionized by Pop III stars (Raiter et al. 2010), so the

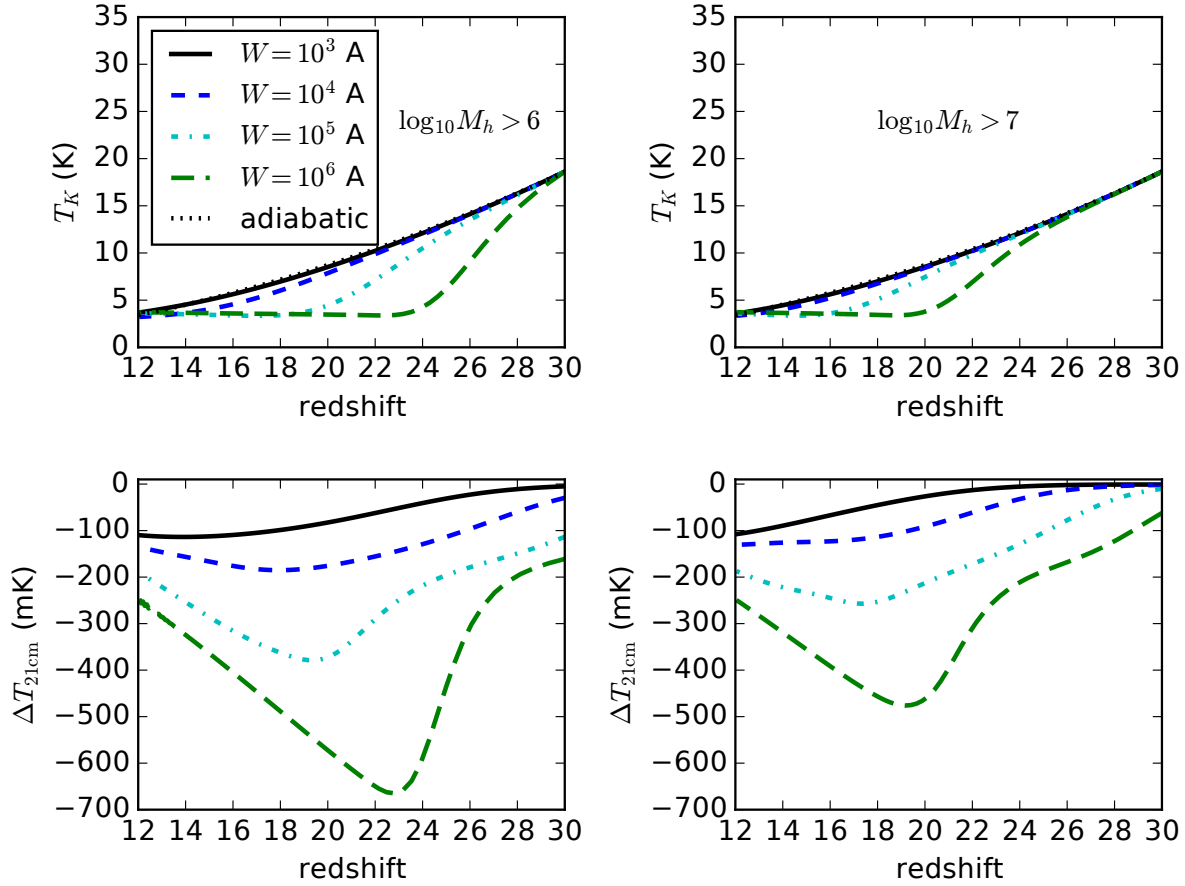


Figure 6. Evolution of the IGM temperature T_K (top panels), and the differential 21-cm antenna temperature $\Delta T_{21\text{-cm}}$ (bottom panels) for emission from haloes with total masses $M_h > 10^6$ (left hand panels) and $10^7 h^{-1} M_\odot$ (right hand panels), with star formation efficiency factor $\epsilon_{\text{SF}} = 0.0003$. Internal scattering through an outflowing region extending to $R_w = 200$ pc and maximum outflow velocity $v_w = 7 \text{ km s}^{-1}$ with a neutral hydrogen density of 10^{-4} cm^{-3} and temperature $T_{\text{ISM}} = 110 \text{ K}$ is assumed. A central Ly α source is assumed present with equivalent widths of $W = 10^3 \text{ \AA}$, 10^4 \AA , 10^5 \AA and 10^6 \AA , considered, as indicated.

higher values considered greatly exceed the expectation from radiative recombinations in photoionized gas. There are no astrophysical models for the origin of such high Ly α equivalent widths; it is noted that other physical mechanisms are available for producing Ly α photons, including the generation of Ly α photons through electron collisional excitation of neutral hydrogen in shock fronts propagating through largely neutral gas and through the impact of soft X-rays in nearly neutral gas followed by excitations by secondary electrons. With a normalizing Ly α equivalent width of 1000 \AA for $\epsilon_{\text{SF}} = 0.0003$, equivalent widths of 10^4 – 10^6 \AA correspond to energy conversion efficiencies of the halo baryons into Ly α photons of approximately 10^{-5} – 10^{-3} . As an example, for accretion onto a black hole the upper end corresponds to a typical black hole energy conversion efficiency of 0.1 – 0.3 .

As shown in the top right hand panel of Fig. 6, intense Ly α emission is able to cool the IGM substantially faster than adiabatic cooling from the expansion of the Universe. Much lower differential 21-cm antenna temperatures are produced, extending to as low as $\Delta T_{21\text{-cm}} \sim -700 \text{ mK}$, with values $\Delta T_{21\text{-cm}} < -300 \text{ mK}$ possible over the redshift range $13 < z < 26$. The signal diminishes towards lower redshift because the Ly α photons eventually heat the gas.

In fact a floor IGM temperature of $T_K = 3.2 \text{ K}$ is found (Fig. 6, upper panels), with Ly α cooling converting to heating at $T_K \lesssim 4 \text{ K}$.

The expanding wind model applies only for radiation in the Lorentz wing of the Ly α scattering cross section. Cooling may also occur for scattering across the Doppler core for a sufficiently red source. This is demonstrated by modelling a reddened emission spectrum from a slab as a double-Gaussian profile of the form

$$\tilde{S}(x) = a_0(1)e^{-[x-x_0(1)]^2/2\sigma_0^2(1)} + a_0(2)e^{-[x-x_0(2)]^2/2\sigma_0^2(2)}, \quad (24)$$

normalized according to

$$\frac{4}{\gamma_S n_\infty} \int_{-\infty}^x dx' \tilde{S}(x') = \left[1 + \text{erf} \left(\frac{x - x_0(1)}{2^{1/2} \sigma_0(1)} \right) \right] + \left[1 + \text{erf} \left(\frac{x - x_0(2)}{2^{1/2} \sigma_0(2)} \right) \right], \quad (25)$$

in agreement with Eq (11) in the absence of a background continuum ($n_\infty = 0$). The line widths correspond to the temperature of the emitting gas. Reddening through a surrounding expanding circum-galactic medium is modelled by assuming an asymmetric profile.

Allowing for the freedom to place the peak of a red pro-

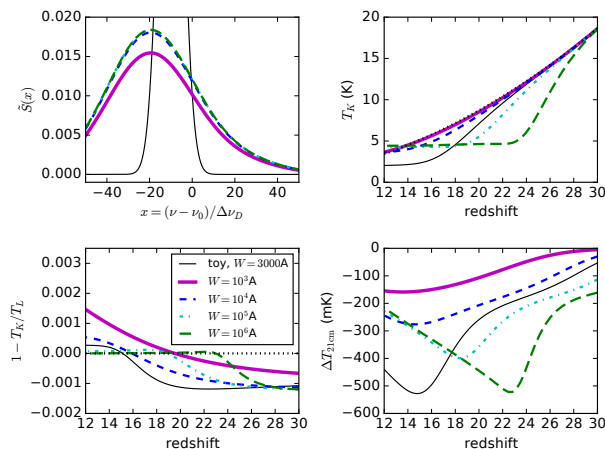


Figure 7. Evolution of IGM temperature including Ly α photon recoil cooling and heating for double-Gaussian source profiles, with initial centres at $\pm 20\Delta\nu_{D,i}$ and initial widths of $20\Delta\nu_{D,i}$, where $\Delta\nu_{D,i}$ is the Doppler width of the IGM at $z_i = 30$. The red-to-blue amplitudes of the Gaussians are in the ratio 10:1. Emission is from haloes with $M_h > 10^6 h^{-1} M_\odot$ and $\epsilon_{\text{SF}} = 0.0003$, and Ly α equivalent widths from $W = 10^3 - 10^6$ Å. Shown are: (upper left) normalized source profiles, (upper right) evolution in IGM kinetic temperature, (lower left) Ly α recoil heating efficiency $1 - T_K/T_L$, (lower right) differential 21-cm antenna temperature. Also shown for comparison are results for a toy model with a sharp Ly α Gaussian source centred at $x = -10$, normalized to $W = 3000$ Å (thin black lines).

file closer to line-centre, we first examine how much cooling may be initiated by a moderate equivalent width emission line. We consider a toy model: a sharp pure red Gaussian profile initially centred at $x_0 = -10$ with an initial width $\sigma_0 = 5$ at $z = 30$. The source is normalized to an equivalent width $W = 3000$ Å for a star formation efficiency $\epsilon_{\text{SF}} = 0.002$, sufficiently low to ensure the associated LyC radiation will not overly photoionize the IGM, assuming a minimum halo mass $M_h > 10^6 h^{-1} M_\odot$ for the sources. As shown in Fig. 7 (thin black lines), strong cooling is achieved, with a minimum 21-cm brightness temperature of $\Delta T_{21-\text{cm}} \sim -500$ mK reached by $z = 15$. The position of the source peak corresponds to an expansion velocity of $\sim 4 \text{ km s}^{-1}$ and the width to thermal broadening of an ISM at 460 K. Such a Ly α source could not be directly generated by radiative recombinations or collisional excitation, although possibly such photons may be generated in cold gas by secondary electrons from X-rays impinging on such cold gas, if such a scenario is workable.

A case with a more plausible ISM temperature is illustrated with an initial $[x_0(1), x_0(2)] = [-20, 20]$ and $\sigma_0(1) = \sigma_0(2) = 20$ at $z = 30$, corresponding to thermally broadened Doppler emission profiles from a medium with temperature $20^2 T_{\text{IGM}}(z_i = 30) = 7400$ K. The Gaussian centres and widths are fixed in physical units. A red-to-blue amplitude ratio 10:1 is assumed. The resulting evolution in gas temperature and differential 21-cm antenna temperature is shown in Fig. 7 for emission from haloes with $M_h > 10^6 h^{-1} M_\odot$, $\epsilon_{\text{SF}} = 0.0003$ and Ly α equivalent widths of $10^3 - 10^6$ Å. Similar evolution in the IGM temperature is found as for the expanding sphere model, with a floor temperature of ~ 4 K before Ly α recoil cooling converts to heating. A

minimum differential 21-cm antenna temperature as low as ~ -500 mK may be reached.

5 DISCUSSION

Full coupling of the 21-cm spin temperature to the IGM temperature, allowing for adiabatic expansion alone of the IGM since the recombination era, produces a differential 21-cm antenna temperature $\Delta T_{21-\text{cm}}$ compared with the CMB ranging from -170 mK at $z = 30$ to -290 mK at $z = 12$. For conventional star formation rate assumptions in the first galaxies, the Ly α intensity is not expected to be sufficiently strong to produce strong coupling between the IGM spin and kinetic temperatures until $z \lesssim 20$, with $\Delta T_{21-\text{cm}} \simeq -10$ mK at $z = 30$, and decreasing to $\Delta T_{21-\text{cm}} < -200$ mK only by $z < 20$ (eg Barkana & Loeb 2005; Hirata 2006).

We consider a broader class of models, allowing for star formation in haloes with minimum masses of $10^6 - 10^7 h^{-1} M_\odot$, and explore a range of assumptions concerning the conversion efficiency of baryons to stars, and the internal gas structure of the haloes. We also consider the enhanced energy production of LyC and Ly α photons in H II regions within primordial galaxies dominated by Pop III stars, following Raiter et al. (2010). Ly α emission equivalent widths of $1000 - 4000$ Å may result, several times larger than predictions for the H II regions of Pop II stars.

For high escape fractions of LyC photons into the IGM, many of the models predict an amount of ionization of the IGM inconsistent with CMB limits on the intergalactic Thomson optical depth. The high escape fractions also result in reduced Ly α photon production within the H II regions of the galaxies. For low escape fractions instead, an intense rate of Ly α production results, sufficient to alter the intergalactic temperature through recoils between Ly α photons and the neutral intergalactic hydrogen.

In the simplest model of a small LyC radiation escape fraction through a static ISM, the H I column density within the H II regions is at least $\sim 10^{18} \text{ cm}^{-2}$. Approximating the radiative transfer through this column density by a static slab model produces two broadly spaced Ly α emission horns emergent from the galaxies. Solving for the intergalactic radiative transfer of the Ly α photons from these galactic sources shows that, for a conservative estimate of the conversion efficiency of baryons to stars, the blue horns produce a strong metagalactic Ly α continuum across line-centre that acts as a heat source through Ly α photon recoils and slows the adiabatic cooling of the IGM. The Ly α metagalactic field more strongly couples the spin temperature to the IGM kinetic temperature than in conventional models. A floor differential antenna temperature of $\Delta T_{21-\text{cm}} \simeq -200$ mK results for this class of models. This is because the heating of the IGM by Ly α recoils eventually causes the 21-cm signal to diminish, producing a characteristic trough in $\Delta T_{21-\text{cm}}$ between $12 < z < 30$. For a minimal halo mass for forming stars of $10^6 h^{-1} M_\odot$, $\Delta T_{21-\text{cm}}$ reaches ~ -200 mK by $z = 21$. For a minimal halo mass of $10^7 h^{-1} M_\odot$, the minimum is not reached until $z \sim 18$, as in conventional models. The redshift for reaching $\Delta T_{21-\text{cm}} \simeq -200$ mK is shifted to earlier epochs for more efficient baryon conversion into stars.

Decreasing the star formation efficiency by an order of

magnitude avoids over-ionizing the IGM without requiring an optically thick H I column density (at the Lyman edge). For a low density ISM, the H II regions can continue to grow without becoming recombination bound. In models in which the interior halo gas expands at velocities comparable to the escape velocity, as may result following a massive supernova explosion, Ly α photons produced by a subsequent episode of star formation would be reddened as they scatter through the expanding halo gas. In such a scenario, much more moderate 21-cm signatures result, comparable to more conventional scenarios for a minimal halo mass for star formation of $10^7 h^{-1} M_{\odot}$. For a minimal halo mass as low as $10^6 h^{-1} M_{\odot}$, $\Delta T_{21-\text{cm}}$ reaches a minimum of ~ -120 mK by $z = 14$. At lower redshifts, the metagalactic Ly α field is sufficiently strong to heat the IGM, reducing the 21-cm signature to $\Delta T_{21-\text{cm}} \simeq -100$ mK by $z = 12$.

At $z > 19$, the models with an expanding interior actually cool the IGM through Ly α photon recoils. Enhancing the Ly α emission equivalent width enhances the cooling. We explore the consequences of models with Ly α emission equivalent widths reaching 10^6 Å. Such extreme values are not predicted from radiative recombinations within any existing models; but neither are such values astrophysically ruled out. Such intensities may be produced through an alternative route, such as collisional excitation within shock fronts or by secondary electrons in neutral gas produced by soft X-rays impinging on the surroundings of the sources. Whether it is possible to achieve such high equivalent widths whilst still producing a predominantly reddened Ly α spectrum or without excessive heating by X-rays in the large scale IGM is unknown.

We show that intense Ly α production with such extreme equivalent widths is able to supercool the IGM, lowering the gas kinetic temperature to a floor of $3 - 4$ K before the Ly α photons begin to heat the gas through recoils. A broad dip in the 21-cm antenna temperature results over redshifts $12 < z < 30$, with a minimum temperature as low as $\Delta T_{21-\text{cm}} \sim -700$ mK. The signature is similar to the measurement reported for the EDGES experiment (Bowman et al. 2018), including a sharp decline as the signature develops, the sharpness increasing as the threshold halo mass for forming stars is increased. This is because the number of haloes grows more rapidly with time the greater the threshold halo mass. Although the signal decreases much more gradually than does the EDGES signal, the signal would decrease more rapidly if additional IGM heating sources formed, such as X-ray emitting compact binaries within the primordial galaxies.

6 CONCLUSIONS

Within the context of conventional models of star formation in primordial galaxies, the differential 21-cm antenna temperature between the IGM and the CMB is expected to lie between $-100 < \Delta T_{21-\text{cm}} < 0$ at $z > 20$. In this paper, we extend the models to explore a broader range of possible 21-cm signatures at these early epochs.

Allowing for enhanced Ly α photon production from Pop III star H II regions (Raiter et al. 2010), we find the Ly α scattering rate P_{α} may exceed the thermalization rate P_{th} required to begin coupling the 21-cm spin tempera-

ture to the gas kinetic temperature as early as redshifts $30 - 25$ for a minimum halo mass for star formation between $10^6 - 10^7 h^{-1} M_{\odot}$. Such high levels of Ly α emission, however, may be accompanied by a metagalactic LyC background sufficiently strong to photoionize the IGM at a level in excess of the CMB limits on the Thomson optical depth.

The excessive reionization may be suppressed in two ways, by exhausting the supply of ionizing photons within recombination-bound H II regions of the primordial galaxies or by reducing the star formation efficiency. We examine both cases. For the latter, we also allow for expanding interior gas within the haloes that may redden the emergent Ly α spectrum, motivated by observations of reddened Ly α spectra (eg Steidel et al. 2010; Heckman et al. 2011), and by models of the impact of supernovae on the gaseous interiors of primordial haloes (Whalen et al. 2008, 2013; Smith et al. 2015).

The Ly α photons produced within a recombination-bound H II region must traverse an H I column density of $\sim 10^{18} \text{ cm}^{-2}$ or more. A characteristic double-horned profile results, displaced by several Doppler widths (referenced to the IGM temperature) to the blue and red of line-centre. The resulting Ly α metagalactic radiation field acts as an additional heating source. The differential 21-cm antenna temperature is then limited to a floor of $\Delta T_{21-\text{cm}} > -200$ mK over $z < 30$. The floor arises because either the Ly α radiation field is not sufficiently strong to fully couple the 21-cm spin temperature to the gas kinetic temperature, or because the radiation field is so strong it heats the IGM through Ly α photon recoils. The result is an extended trough in the differential antenna temperature over the redshift range $12 < z < 30$.

Lowering the star formation efficiency, as may be expected in the presence of substantial feedback, diminishes the strength of the 21-cm absorption signature, in agreement with previous estimates. Allowing for reddening within an expanding halo, however, produces net cooling by Ly α photon recoils, even accounting for the accompanying continuum-produced Ly α photons, which always heat the gas. For plausible Ly α emission line equivalent widths of primordial H II regions, limited to < 4000 Å, the amount of cooling is small, producing less than a 5 percent decrease in the IGM kinetic temperature compared with the reduction by adiabatic expansion cooling since the recombination era. By $z < 19$, continuum Ly α heating dominates and the IGM begins to warm. The effect is again a dip in the differential 21-cm antenna temperature, with a minimum $\Delta T_{21-\text{cm}} > -150$ mK between $12 < z < 18$, depending on the minimum halo mass for star formation.

Motivated by the large absorption signature reported from the EDGES experiment of $\Delta T_{21-\text{cm}} \simeq -650 - -450$ mK between $16 < z < 19$ (Bowman et al. 2018), we also consider models that may supercool the IGM. Whilst sources emitting to the red of line-centre with moderate equivalent widths may produce brightness temperatures as low as $\Delta T_{21-\text{cm}} \sim -500$ mK, they require narrow widths corresponding to ISM temperatures much smaller than 10^4 K; a mechanism for producing Ly α photons in such cold gas is problematic. Warmer ISM temperatures require instead extreme Ly α emission equivalent widths for supercooling, up to 10^6 Å, in expanding halo gas. We find deep absorption signatures of up to -700 mK are achievable for these

models, with a broad trough where $|\Delta T_{21-\text{cm}}| < 300$ mK over $13 < z < 26$. As the redshift decreases, heating by Ly α recoils dominates, decreasing the strength of the absorption signal to $|\Delta T_{21-\text{cm}}| < 250$ mK by $z = 12$. An astrophysical model that would produce the required high Ly α emission equivalent widths, however, remains elusive.

APPENDIX A: CONSTRAINTS ON Ly α PHOTON SCATTERING RATE FROM REIONIZATION LIMITS

The production rate $Q(H)$ of LyC photons, allowing for an escape fraction f_{esc} , is related to \dot{n}_α by

$$Q(H) = \frac{\dot{n}_\alpha}{(1 - f_{\text{esc}})P\bar{f}_{\text{coll}}}, \quad (\text{A1})$$

where P is an energy enhancement factor, increasing with hardness of the stellar spectrum and the gas density of the H II region and ranging over $1 \lesssim P \lesssim 4$ (Raiter et al. 2010). The relative number of Ly α photons produced per recombination is quantified by f_{coll} , with $2/3 \lesssim f_{\text{coll}} \lesssim 1$. For a small escape fraction $f_{\text{esc}} \ll 1$, $2/3 < Q(H)/\dot{n}_\alpha < 4$, so that the cumulative numbers of Ly α and LyC photons produced are comparable. The LyC photons are largely confined to the H II regions, producing Strömgren spheres, with recombinations balancing photoionizations. For an assumed source spectrum varying as $\nu^{-\alpha_S}$, the photoionization rate per hydrogen atom at a distance r from the source is $\Gamma_i \simeq [\alpha_S/(3 + \alpha_S)]Q(H)\sigma_L/(4\pi r^2)$, where σ_L is the photoelectric cross section at the ionization threshold energy. For a uniform density gas, the accumulated H I column density through the Strömgren sphere is then

$$N_{\text{HI}}^{\text{Str}} \approx \frac{3 + \alpha_S}{\alpha_S} \frac{1}{\sigma_L} \approx 10^{18} \text{ cm}^{-2}. \quad (\text{A2})$$

For a characteristic temperature $T = 10^4 T_4$ K for photoionization heated gas, the line centre optical depth for Ly α scattering is $\tau_\alpha \simeq 6 \times 10^4 T_4^{-1/2}$. The Ly α photons escape the H II region by diffusing in frequency until the H II region is optically thin to Ly α photon scattering.

For larger escape fractions, the stars begin to photoionize the IGM, with photons entering the IGM at the rate $Q_{\text{IGM}}(H) = f_{\text{esc}}Q(H)$, so that

$$Q_{\text{IGM}}(H) = \frac{f_{\text{esc}}}{(1 - f_{\text{esc}})P\bar{f}_{\text{coll}}} \dot{n}_\alpha. \quad (\text{A3})$$

The number density of LyC photons is then related to the total number density n_α of Ly α photons produced by $n_L = f_{\text{esc}}n_\alpha/[(1 - f_{\text{esc}})P\bar{f}_{\text{coll}}]$. For $f_{\text{esc}} = 0.2$, for example, if $n_\alpha > \bar{n}_H$, where \bar{n}_H is the mean IGM hydrogen density, a substantial fraction of the IGM will have been photoionized.² This may conflict with CMB limits on the Thomson optical depth. For a 1σ (2σ) upper limit of $\tau_e < 0.06$ (0.07) (Planck Collaboration 2018), the additional contribution to the optical depth must be limited to $\Delta\tau_e < 0.02$ (0.03) after subtracting the contribution between $z = 0$ and 6. As shown in Fig. 1 (for $P\bar{f}_{\text{coll}} = 2$), this limit may be reached for a

² Recombinations within a clumped IGM will slow the reionization process, but this is expected to produce only a small to moderate delay (eg Shull et al. 2012; D’Aloisio et al. 2020).

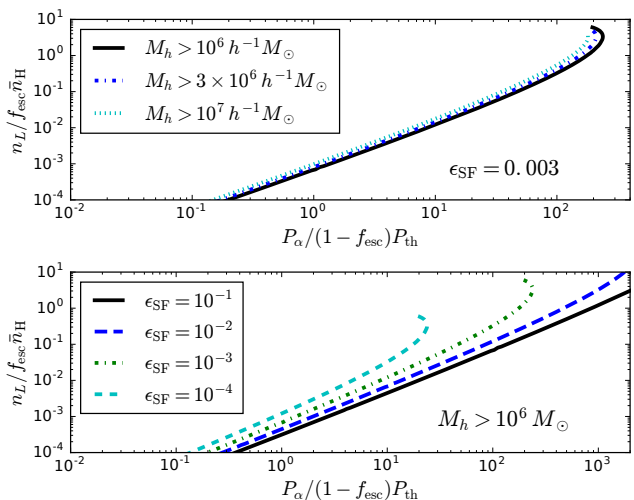


Figure A1. The integrated number density n_L of LyC photons produced in the IGM for $f_{\text{esc}} > 0$, normalized by the total hydrogen density, against the Ly α scattering rate P_α , normalized by the thermalization rate P_{th} . The top panel shows the variation for different minimum halo mass threshold values for star formation, and the bottom panel shows the dependence on nuclear star formation efficiency ϵ_{SF} for a halo mass threshold $M_h > 10^6 h^{-1} M_\odot$.

minimum halo mass for star formation of $M_h > 10^6 h^{-1} M_\odot$ at $z < 13$, assuming the number density of ionized hydrogen and singly ionized helium atoms matches n_L . Since $\tau_e \bar{n}_H / n_L$ generally exceeds 0.01 at $z < 35$, (bottom right hand panel of Fig. 1), once $n_L > \bar{n}_H$, the Thomson optical depth will have reached 0.01. The IGM may thus become close to being fully photoionized before exceeding the CMB limit. The emission of LyC radiation from galaxies, however, will have to abruptly cease to allow the ionized gas to recombine to avoid exceeding the CMB limit. At $z = 15$, the recombination time of 10^4 K is too long, of order 100 Myr, corresponding to an additional increment $\Delta\tau_e \approx 0.04$. The Compton cooling time, however, is very short, a little under 35 Myr. Upon cooling to the CMB temperature, the gas will quickly recombine. The incremental increase in the optical depth is then only $\Delta\tau_e \approx 0.017$ if fully ionized. It would thus be possible for about half of the IGM to become ionized briefly by $z = 15$ without exceeding the CMB limit on the Thomson optical depth. More generally, however, at higher redshifts $n_L/\bar{n}_H \lesssim 0.5$ is required to ensure the CMB limit is not exceeded.

From Fig. A1 (upper panel), for an escape fraction $f_{\text{esc}} < 0.2$, requiring $n_L/\bar{n}_H < 0.5$ imposes the restriction $P_\alpha/P_{\text{th}} \lesssim 200$ for $\epsilon_{\text{SF}} = 0.003$. Even for the extreme efficiency $\epsilon_{\text{SF}} = 0.1$, the cumulative number of ionization proceeds much more quickly and Fig. A1 (lower panel) shows $P_\alpha/P_{\text{th}} < 3000$ (at an earlier epoch) is required. For $\epsilon_{\text{SF}} = 10^{-4}$, the limit could be as low as $P_\alpha/P_{\text{th}} < 20$. The limits become even more severe for higher escape fractions.

APPENDIX B: CONTRIBUTION FROM HIGHER ORDER LYMAN PHOTONS

The direct scattering rate of higher order Ly- n photons is

$$P_n^{\text{dir}} = P_n^{\text{inc}}(0)\mathcal{S}_n, \quad (\text{B1})$$

where $P_n^{\text{inc}}(0) = \sigma_n L_{\nu_n} / (4\pi r_L^2 h\nu_n)$ is the scattering rate assuming no intergalactic attenuation, r_L is the luminosity distance from a source with specific luminosity L_{ν_n} at the Ly- n transition frequency ν_n , and where σ_n is the total Ly- n resonance cross section. Intergalactic attenuation is accounted for by the suppression factor \mathcal{S}_n . To good approximation, $\mathcal{S}_n \gtrsim \gamma_n$, where $\gamma_n = H(z)/[\lambda_n \sigma_n n_{\text{HI}}(z)]$ is the Sobolev parameter for the Ly- n transition of wavelength λ_n , $H(z)$ is the Hubble parameter at redshift z , and $n_{\text{HI}}(z)$ is the mean intergalactic neutral hydrogen density (Meiksin 2010; Kakiichi et al. 2012). In addition to direct scatters, higher order Lyman photons will generate lower order Lyman photons through radiative cascades. The net scattering rate of higher Lyman photons may be expressed as

$$P_n = \frac{1}{1 - p_{nn}} \sum_{n'=n}^{n_{\text{max}}} C_{n'n} P_{n'}^{\text{dir}}, \quad (\text{B2})$$

where the scattering cascade matrix is given by

$$C_{n'n} = \sum_{n''>n}^{n'} C_{n'n''} \eta_{n''n}, \quad (\text{B3})$$

where $C_{nn} = 1$, $C_{n'n} = 0$ for $n > n'$ and $\eta_{n'n} = p_{n'n}/(1 - p_{n'n})$, where $p_{n'n}$ is the probability for a Ly- n' photon to convert into a Ly- n photon on scattering (Meiksin 2010; Kakiichi et al. 2012). For the special case of Ly α photons,

$$P_\alpha = P_\alpha^{\text{inc}}(0) + \mathcal{N}_{\text{scatt}} \sum_{n'=2}^{n_{\text{max}}} C_{n'2} P_{n'}^{\text{dir}}, \quad (\text{B4})$$

and $\mathcal{N}_{\text{scatt}} = 1/\gamma_S$ is the number of scatters a Ly α photon undergoes in the IGM before redshifting sufficiently far into the Lorentz wing to escape.

The total heating rate per unit volume due to the scattering of Ly- n photons ($n > 2$) at rate P_n per neutral hydrogen atom is

$$G_n = P_n n_{\text{HI}} \frac{h\nu_n}{m_a c^2} \sum_{n'=1}^{n-1} \frac{A(n, 1; n', 0) + A(n, 1; n', 2)}{A_{n,1}} \times h\nu_{nn'} \left(1 - \frac{T_K}{\langle T_{nn'} \rangle_{\text{H}}} \right), \quad (\text{B5})$$

for an IGM kinetic temperature T_K and harmonic mean light temperature

$$\langle T_{nn'} \rangle_{\text{H}} = \frac{\nu_{nn'}}{\nu_n} \frac{\int_0^\infty d\nu n_\nu \varphi_V(a_n, \nu)}{\int_0^\infty d\nu \frac{1}{T_n(\nu)} n_\nu \varphi_V(a_n, \nu)}, \quad (\text{B6})$$

where

$$T_n(\nu) = -\frac{h}{k} \left(\frac{d \log n_\nu}{d\nu} \right)^{-1} \quad (\text{B7})$$

for a photon number density n_ν (Meiksin 2010). Here $\nu_{nn'} = \nu_L(1/n'^2 - 1/n^2)$ (and $\nu_n = \nu_{n1}$), where ν_L is the frequency of the Lyman edge. $A_{n,1}$ is the total decay rate of the p -state with principal quantum number n . (Note $A(n, 1; n', 2)$ is undefined for $n' < 3$, and should be regarded as zero.)

A given position in the IGM at redshift z will receive Ly- n photons only from within a restricted redshift range given by

$$1 + z_n^{\text{hor}} = (1 + z) \frac{1 - (n+1)^{-2}}{1 - n^{-2}}, \quad (\text{B8})$$

as photons emitted from greater distances that would have redshifted to Ly- n will instead be scattered by the Ly- $(n+1)$ transition of a neutral hydrogen atom along the way (Barkana & Loeb 2005). For a comoving source luminosity function $\Phi(L)$, representing the number of sources per unit volume with luminosity between L and $L + dL$, the total direct scattering rate for Ly- n photons is

$$\begin{aligned} P_n^{\text{dir, Tot}} &= \int_z^{z_n^{\text{hor}}} dz \frac{dr_p}{dz} (1+z)^3 4\pi r_p^2 \\ &\times \int_0^\infty dL_{\nu_n} \frac{\sigma_n L_{\nu_n}}{4\pi r_L^2 h\nu_n} \mathcal{S}_n \Phi(L_{\nu_n}) \\ &\simeq \int_z^{z_n^{\text{hor}}} dz \frac{dr_p}{dz} (1+z)^3 \frac{\sigma_n \epsilon_n}{h\nu_n} \mathcal{S}_n(z), \end{aligned} \quad (\text{B9})$$

where $\epsilon_n = \int dL_{\nu_n} L_{\nu_n} \Phi(L_{\nu_n})$ is the comoving source emissivity, and the luminosity distance r_L is approximated as the proper distance r_p . A similar expression applies for $P_\alpha^{\text{dir, Tot}}$, with $\mathcal{S}_2 = 1$. To good approximation, $P_n^{\text{dir, Tot}}$ may be used in Eq. (B5) to obtain the total Ly- n heating rate from all sources since $\langle T_{nn'} \rangle_{\text{H}}$ is nearly independent of source distance (Meiksin 2010), although it is straightforward to integrate over sources as in Eq. (B9) if preferred, and is done for the results presented here.

ACKNOWLEDGMENTS

AM acknowledges support from the UK Science and Technology Facilities Council, Consolidated Grant ST/R000972/1. P.M. acknowledges a NASA contract supporting the WFIRST-EXPO Science Investigation Team (15-WFIRST15-0004), administered by GSFC.

REFERENCES

- Barkana R., Loeb A., 2005, ApJ, 626, 1
- Blumenthal G. R., Faber S. M., Primack J. R., Rees M. J., 1984, Nature, 311, 517
- Bond J. R., Szalay A. S., 1983, ApJ, 274, 443
- Bowman J. D., Rogers A. E. E., Monsalve R. A., Mozdzen T. J., Mahesh N., 2018, Nature, 555, 67
- Chen X., Miralda-Escudé J., 2004, ApJ, 602, 1
- Chuzhoy L., Shapiro P. R., 2006, ApJ, 651, 1
- Couchman H. M. P., Rees M. J., 1986, MNRAS, 221, 53
- D'Aloisio A., McQuinn M., Trac H., Cain C., Mesinger A., 2020, arXiv e-prints, p. arXiv:2002.02467, 2002.02467
- Dijkstra M., Mesinger A., Wyithe J. S. B., 2011, MNRAS, 414, 2139
- Field G. B., 1958, Proc. I.R.E., 46, 240
- Field G. B., 1959, ApJ, 129, 536
- Field G. B., 1964, ApJ, 140, 1434
- Haiman Z., Rees M. J., Loeb A., 1997, ApJ, 476, 458
- Harrington J. P., 1973, MNRAS, 162, 43
- Heckman T. M., Borthakur S., Overzier R., Kauffmann G., Basu-Zych A., Leitherer C., Sembach K., Martin D. C., Rich R. M., Schiminovich D., Seibert M., 2011, ApJ, 730, 5

- Higgins J., Meiksin A., 2009, MNRAS, 393, 949
Higgins J., Meiksin A., 2012, MNRAS, 426, 2380
Hirata C. M., 2006, MNRAS, 367, 259
Kakiichi K., Meiksin A., Tittley E., 2012, MNRAS, 426, 2129
Loeb A., Rybicki G. B., 1999, ApJ, 524, 527
Madau P., 2018, MNRAS, 480, L43
Madau P., Meiksin A., Rees M. J., 1997, ApJ, 475, 429
Mason C. A., Treu T., Dijkstra M., Mesinger A., Trenti M., Pentericci L., de Barros S., Vanzella E., 2018, ApJ, 856, 2
Meiksin A., 2006, MNRAS, 370, 2025
Meiksin A., 2010, MNRAS, 402, 1780
Meiksin A., 2011, MNRAS, 417, 1480
Ono Y., Ouchi M., Mobasher B., Dickinson M., Penner K., Shimasaku K., Weiner B. J., Kartaltepe J. S., Nakajima K., Nayyeri H., Stern D., Kashikawa N., Spinrad H., 2012, ApJ, 744, 83
Partridge R. B., Peebles P. J. E., 1967, ApJ, 147, 868
Planck Collaboration 2018, ArXiv e-prints, 1807.06209
Raiter A., Schaerer D., Fosbury R. A. E., 2010, A&Ap, 523, A64
Reed D. S., Bower R., Frenk C. S., Jenkins A., Theuns T., 2007, MNRAS, 374, 2
Rybicki G. B., 2006, ApJ, 647, 709
Rybicki G. B., dell’Antonio I. P., 1994, ApJ, 427, 603
Schauer A. T. P., Glover S. C. O., Klessen R. S., Ceverino D., 2019, MNRAS, 484, 3510
Schenker M. A., Ellis R. S., Konidakis N. P., Stark D. P., 2014, ApJ, 795, 20
Seager S., Sasselov D. D., Scott D., 2000, ApJS, 128, 407
Shull J. M., Harness A., Trenti M., Smith B. D., 2012, ApJ, 747, 100
Smith A., Safrank-Shrader C., Bromm V., Milosavljević M., 2015, MNRAS, 449, 4336
Smith B. D., Wise J. H., O’Shea B. W., Norman M. L., Khochfar S., 2015, MNRAS, 452, 2822
Stark D. P., Ellis R. S., Chiu K., Ouchi M., Bunker A., 2010, MNRAS, 408, 1628
Steidel C. C., Erb D. K., Shapley A. E., Pettini M., Reddy N., Bogosavljević M., Rudie G. C., Rakic O., 2010, ApJ, 717, 289
Tinsley B. M., 1972, ApJ, 178, 319
Truran J. W., Cameron A. G. W., 1971, ApSS, 14, 179
Tseliakhovich D., Hirata C., 2010, PhysRevD, 82, 083520
Verhamme A., Dubois Y., Blaizot J., Garel T., Bacon R., Devriendt J., Guiderdoni B., Slyz A., 2012, A&Ap, 546, A111
Visbal E., Barkana R., Fialkov A., Tseliakhovich D., Hirata C. M., 2012, Nature, 487, 70
Whalen D., van Veelen B., O’Shea B. W., Norman M. L., 2008, ApJ, 682, 49
Whalen D. J., Johnson J. L., Smidt J., Meiksin A., Heger A., Even W., Fryer C. L., 2013, ApJ, 774, 64
Wouthuysen S. A., 1952, AJ, 57, 31
Yoshida N., Abel T., Hernquist L., Sugiyama N., 2003, ApJ, 592, 645
Zanstra H., 1949, Bull. Ast. Insts. Neth., 11, 1